An idealized long–term morphodynamic model of a tidal embayment

H.M. Schuttelaars *
Mathematical Institute, Utrecht University,
P.O.Box 80.010, 3508 TA Utrecht, The Netherlands

H.E. de Swart
Institute for Marine and Atmospheric Research, Utrecht University,
P.O.Box 80.000, 3508 TA Utrecht, The Netherlands

May 15, 1997

Abstract

A model is discussed which describes the interaction between tidal currents, sediment transport and bedform changes in a one dimensional short embayment with a constant width. The water motions are described by the depth–integrated shallow water equations. They are forced by prescribed free surface elevations at the entrance which consist of a basic tide and a first overtide. For the sediment dynamics both a bedload and a suspended load transport model are considered. The sediment balance is averaged over a tidal period to retain only the long–term behaviour of the bottom profile.

The equilibrium profiles are calculated and the stability properties of these profiles are studied for various combinations of the model parameters. If the forcing does not contain overtides the suspended load model has a unique stable equilibrium which represents a constantly sloping bottom with zero depth at the closed end and spatially uniform tidal currents. In contrast the equilibrium profile of the bedload model is a flat bottom. The introduction of overtides in the forcing results in more complex dynamics. The equilibrium bottom profiles in the suspended load model can be convex or concave, depending on the ratio of advective and diffusive transports. Solutions of the bedload model tend to a bottom of constant slope where the water depth at the closed end may be finite. A physical interpretation of these results is also given.

*This research was supported by NWO–grant nr. NLS 61-261. Furthermore, we thank A. van Harten, A. Doelman and C.T. Friedrichs for their comments on earlier versions of this paper.

1 Introduction

From various points of view (coastal protection, water and bottom quality, ecology, etcetera) tidal estuaries and basins are very important elements of the coastal system. Due to prevailing currents, generated by tides, wind and density differences, the bottom in these areas tends to develop channels and shoals. These morphological changes in turn have a significant effect on the flow dynamics and hence on the general tendency of the tidal embayment to import or export sediment (Aubrey & Speer, 1985; Speer & Aubrey, 1985). Besides, the shoals as well as the channels are of paramount importance to the ecosystem (Jonge, 1992). The bottom evolution in such areas is the result of a delicate balance between large in– and outgoing fluxes of sediment. This balance can easily be disturbed by external factors, such as extreme storm events, mean sea–level rise, changes in the tidal regime, human interferences, etcetera. A better quantitative explanation of these morphological processes is required in order to be able to understand and predict quasi–stable and transient bottom topographies, and to investigate their sensitivity to changing external conditions.

Although tidal basins and estuaries have been widely investigated during the past decades, the mathematical–physical modelling of the combined interactions between currents and changing bottom topographies is still at an initial stage. Many studies focused on the derivation of empirical relationships between various morphological parameters of the system (Bruun & Gerritsen, 1960), but no dynamical interpretation of these results was given.

Most theoretical studies (Speer & Aubrey, 1985; Parker, 1991; Friedrichs & Aubrey, 1994) were concerned with the dynamics of currents induced by tides, without considering the feedback to morphology. However, it was demonstrated in (Zimmerman, 1981) that the effect of bottom topography on tidal motions is to generate residual currents and overtides, which turn out to have a large impact on the mixing properties of such systems (Ridderinkhof & Zimmerman, 1992). This is not only relevant for the transport of pollutants and nutrients, but also for the transport of fine sediment. Although the expertise and knowledge gathered is useful it is still unclear which fundamental mechanisms cause the morphological evolutions observed in such models. Moreover, due to computer storage problems and pronounced numerical instabilities it is not possible to carry out long–term simulations. These limitations motivate supplementary research on idealized models in which specific physical processes are isolated and which are simple enough to be investigated by analytical methods. It is hoped that the study of such models may contribute to a better understanding of the behaviour of more complicated models as well as observed bed form evolutions.

In the present paper a simple morphodynamic model of a tidal embayment will be developed and analyzed. In particular the relation between dynamical mechanisms and the bed form patterns predicted by this model will be investigated. The organization of this paper is as follows. In section 2 the model equations and boundary conditions are introduced. A schematized rectangular embayment is considered where only its bottom is an erodible boundary. Since tidal basins are very shallow, the full equations of motion may be approximated by the shallow water equations. Here we shall consider their depth–integrated version which implies that we neglect baroclinic effects. The sediment transport model considered describes both bedload transport and transport resulting from suspended load processes. It appears that the time scales of the morphological phenomena (evolution of the channel–shoal system) are much larger than the characteristic flow time scale (the tidal period). This implies that in the analysis use can be made of the method of averaging (Sanders & Verhulst, 1985). Essentially it means that flow and bottom dynamics are treated separately, whereas only the tidally averaged sediment fluxes govern the slow evolution of the bed. Since the width of the embayment is assumed to be small compared to both its length and the Rossby deformation radius, a one dimensional model can be derived. In this model no width variations are considered, as studied in (Friedrichs & Aubrey, 1994). Furthermore, it is assumed that the length of the tidal embayment is much smaller than the tidal wave–length such that the system is far from resonance. Hence, the tidal forcing can be externally described, *i.e.*, the interaction between the tidal embayment and the adjacent sea may be neglected (Garret, 1975). Moreover it implies that the free surface elevations are spatially uniform, which simplifies the analysis considerably. Although the short embayment condition is rather severe, there are natural systems, such as the Dutch Wadden inlets, where it is marginally obeyed. In section 3 the prescribed tidal forcing consists of the leading tidal constituent only. Using this forcing, equilibrium bottom profiles are derived for both the bedload and the suspended load transport formulation. Results of numerical simulations are presented which describe the evolution from a flat bottom to the equilibrium profile. Furthermore, the time scales associated with the different processes are obtained and discussed. The stability of the bottom profiles is investigated, resulting in explicit expressions for both the perturbations and the growth rates of these disturbances. It turns out that the equilibrium profiles are stable within the context of the one dimensional model.

In section 4 the prescribed tidal forcing is given by the basic tide and the first overtide. In this case, even this idealized model already turns out to be very complicated. It must be decided which terms represent the leading order sediment transport contributions. To make this decision, characteristic parameters as found in real embayments are used. Next, equilibrium profiles are obtained analytically. These profiles are found by numerical integration of the bottom evolution equation as well. The stability of these equilibria is investigated. Using variational techniques, the stability of these equilibrium profiles can be determined. In some special cases, the perturbations and their associated growth rates can be written down explicitly. It turns out that even if an overtide is introduced, all equilibria are stable.

In the last section, the results are recapitulated and the two transport models (bedload and suspended load) are compared. Some suggestions for further investigations are made.

2 Model Formulation

2.1 Geometry and Model

The geometry that will be considered is that of an idealized tidal embayment of rectangular shape (width B and length L), ignoring width variations that often strongly constrain the dynamics (Friedrichs & Aubrey, 1994). The coast-lines are assumed to be fixed whereas the bottom (described by $z = -H + h$, with H a reference depth) is erodible. The free surface is described by $z = \zeta$ (see figure 1). The water motions

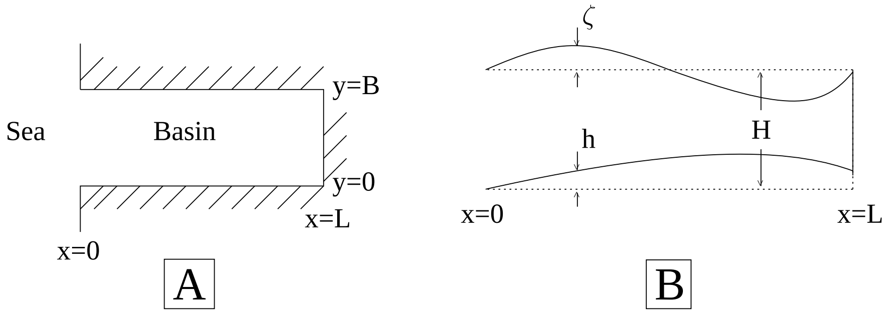

Figure 1: Situation sketch: top view [A] and cross–sectional view [B] of the tidal embayment.

are described by the depth–averaged shallow water equations for a homogeneous fluid (Csanady, 1982). When studying a suspended load model this set of equations must be supplemented with a depth-averaged concentration equation (Rijn, 1993) which describes sediment fluxes due to both advective and diffusive processes and the bottom evolution equation. In case of a bedload model (Dyer, 1986; Rijn, 1993) only the bottom evolution equation is required. As boundary conditions the free surface elevation at $x = 0$ is prescribed and we require that there is no normal water and sediment transport at solid boundaries.

As reported by (Wang *et al.*, 1992), the morphological time scales are much longer than the tidal time scales. For example, in the Friesche Zeegat, one of the tidal embayments in the Dutch Wadden Sea, the typical time scale on which bed forms evolve is of the order of 20 years. The bottom profile only changes on the slow morphological time scales T_s and T_b which are the characteristic time scales of bottom changes due to suspended load and bedload transport, respectively. Therefore, on the short tidal time scale, the bottom h may be considered constant in time. The slow evolution of the bed is not directly determined by the sediment transport within a tidal cycle, but rather by the net, *i.e.* tidally averaged sediment fluxes if the driving tides ζ all have a commensurate period. The mathematical foundations of this approach are discussed in (Sanders & Verhulst, 1985; Krol, 1991). In the present case, this implies that the bottom profile h is only a function of a slow morphological time variable τ, which will be defined later. Averaging theory guarantees that the averaged bottom evolution equation is a good approximation of the original bottom equation at the morphological time scale.

It appears that it is difficult to obtain analytical solutions of the model equations formulated so far. However, as shown in for example (Csanady, 1982), it turns out that in the case of a narrow channel ($B \ll R$ and $B \ll L$, where R is the Rossby deformation radius) our system of equations may be reduced to a one–dimensional model in which no variations in the cross–channel directions are present. The resulting continuity equation is given by

$$\zeta_t + [(H + \zeta - h)u]_x = 0 \tag{1}$$

As a boundary condition we prescribe ζ at $x = 0$, which will represent tidal motions with a characteristic frequency σ, to be specified in section 2.2. In this paper a strongly reduced momentum equation is used, which reads

$$\zeta_x = 0 \tag{2}$$

It models a spatially uniform variation of the free surface which is fully determined by the boundary condition at the entrance. The momentum equation (2) is valid if the embayment length is much smaller than the tidal wave–length and if the frictional time scale is at least of the same order as the tidal period. These conditions are rather severe as the dynamics of many tidal embayments are highly affected by frictional terms (Friedrichs & Madson, 1992). However, there are examples of relatively deep embayments, such as the main channel of the Frisian inlet system, where these conditions are marginally satisfied. As boundary condition, we require that the normal water flux at the fixed boundary vanishes.

We assume that the sediment in the embayment is noncohesive and may be transported both as suspended load and bedload. The transport due to whirling up and settling of the finer sediment particles is called suspended load transport, the transport due to rolling and saltating of coarser sediment particles in a thin active layer is called bedload transport. Roughly stated, suspended load transport occurs if $u_\star > w_{\rm s} > u_{\star\rm c}$, where $u_\star$ is the friction velocity, $w_{\rm s}$ the settling velocity of sediment particles and $u_{\star\rm c}$ the critical friction velocity for erosion. Bedload transport if $w_{\rm s} > u_\star > u_{\star\rm c}$. A derivation of $u_{\star\rm c}$ can be found in (Dyer, 1986; Fredsoe & Deigaard, 1992). The former mechanism is described by the depth–integrated concentration equation

$$C_t + (uC - \mu_\star C_x)_x = S \equiv \alpha u^2 - \gamma C \tag{3}$$

For a derivation see (Rijn, 1993). Here C is the depth–integrated sediment concentration, *i.e.*, the amount of sediment stored in a column sea water with unit horizontal area and $\mu_\star$ is a constant diffusion coefficient. Here the function S describes the sedimentation at the top of the active layer. The first contribution to S models the whirling up of sediment, where α is a coefficient related to sediment properties (grain size, shape, etc.). This parameterization is motivated by the analysis of field observations reported by (Dyer & Soulsby, 1988), see also (Fredsoe & Deigaard, 1992). Typical values of α are $\mathcal{O}(10^{-2}$–$10^{-4}\text{kgsm}^{-4})$ corresponding to fine and medium sand, respectively.

The term $-\gamma C$ models the deposition of the sediment. The constant γ can be related to the settling velocity and a diffusion coefficient κ_v that describes the mixing of the sediment in the vertical. Assuming a constant κ_v it follows from (Rijn, 1993) that $\gamma = w_\mathrm{s}^2/\kappa_\mathrm{v}$. The boundary conditions for the concentration equation are that the normal component of the sediment flux is zero at solid walls. Furthermore, it is imposed that at the entrance of the embayment no diffusive boundary layer should develop. Thus near $x = 0$ the solution for C in the limit $\mu_\star \to 0$ should be consistent with the solution of the concentration equation (3) with $\mu_\star = 0$. This condition yields only information in case the bed level at the entrance is known. Here we require that outside the open boundary there is no net sedimentation, hence $h_t = 0$ at $x = 0$. This condition ensures that we are studying the entire region where the bottom profile changes.

The bottom evolution equation can be derived from continuity of mass in the sediment layer and reads

$$\rho_\mathrm{s}(1-p)\left(h_\tau + \langle S_{\mathrm{b},x}\rangle\right) = -\langle S\rangle \tag{4}$$

with ρ_s the density of the individual grain particles, p the bed porosity and $< \cdot >$ denoting tidal average. The sedimentation function S is defined in (3). Furthermore, S_b is the volumetric sediment flux in the active layer. A parameterization of the bedload model motivated by results presented in (Dyer, 1986; Rijn, 1993) is used:

$$S_\mathrm{b} = \hat{s}\frac{|\boldsymbol{u}|^b}{u_\mathrm{c}^b}\left(\frac{u}{|\boldsymbol{u}|} - \kappa_* h_x\right) \tag{5}$$

for some $b > 1$ and $\kappa_* > 0$. Here u_c is the critical velocity for erosion which, for fine sand, is of the order of 0.3 m s^{-1}. Typical values for b and κ_* are $b \sim 3$ and $\kappa_* \sim 2$, see (Rijn, 1993). The parameter $\hat{s}$ is a function of the sediment properties. From dimensional arguments it follows that $\hat{s} = \mathcal{O}\left(\sqrt{g' d_s^3}\right)$ where $g' = (\rho_s - \rho)g/\rho$ denotes reduced gravity, d_s the sediment diameter. Typical values of $\hat{s}$ are $\mathcal{O}(10^{-6}$–$10^{-4}\text{m}^2\text{s}^{-1})$ for fine and medium sand, respectively (see (Dyer, 1986; Fredsoe & Deigaard, 1992; Rijn, 1993)). The diffusive term measured by the coefficient $\kappa_\star$ is a bed slope correction term which models the preferred downhill transport of sediment. The corresponding boundary condition is that $S_\mathrm{b} = 0$ at the solid boundary $x = L$. In order to solve the model an initial bottom profile should be given. For the other state variables no initial conditions are necessary as we are looking for nontransient solutions on the short tidal time scale.

2.2 Scaling; Nondimensional Model

The equations of motion are made dimensionless by introducing the following transformations:

$$x = Lx^*, t = t^*\sigma^{-1}, u = Uu^*$$
$$\zeta = \frac{HU}{\sigma L}\zeta^*, C = \frac{\alpha U^2}{\gamma}C^*, h = Hh^* \tag{6}$$

The asterix refers to nondimensional variables and U is a velocity scale related to the tidal forcing (with frequency σ) at the entrance of the embayment. The scale for the free surface elevations follows from mass conservation arguments: the first two terms in the continuity equation should be of the same order. The scale for the concentration is obtained from (3) by requiring an approximate balance between the erosion and deposition mechanisms. After suppressing the asterix the nondimensional equations of motion read

$$\zeta_t + [(\epsilon\zeta + 1 - h)u]_x = 0 \tag{7}$$
$$\zeta_x = 0 \tag{8}$$
$$a[C_t + (\epsilon uC - \mu C_x)_x] = u^2 - C \tag{9}$$
$$h_t = -F_x \tag{10}$$

where

$$F = \delta_{\mathrm{s}} a \left[\epsilon \langle uC\rangle - \mu \langle C\rangle_x\right] + \delta_{\mathrm{b}} \left\langle \left[|u|^b \left(\frac{u}{|u|} - \kappa h_x\right)\right]\right\rangle \tag{11}$$

is the net sediment flux. The nondimensional parameters in these equations are

$$\epsilon = \frac{U}{\sigma L}, a = \frac{\sigma}{\gamma}, \mu = \frac{\mu_\star}{\sigma L^2}$$
$$\kappa = \frac{H\kappa_*}{L}, \delta_{\mathrm{s}} = \frac{\alpha U^2}{\rho_{\mathrm{s}}(1-p)H\sigma}, \delta_{\mathrm{b}} = \frac{\hat{s}}{\sigma H L}\left(\frac{U}{u_{\mathrm{c}}}\right)^b \tag{12}$$

Here ϵ is, apart from a factor of 2π, the ratio of the tidal excursion (the distance traveled by a fluid particle in a tidal period) and the tidal inlet length. Furthermore, a is the ratio of the timescale of the deposition process and the tidal period, μ is the ratio of the tidal period and the diffusive time scale and κ measures the effect of bed slope corrections in the bed load sediment flux. The parameters δ_{s} and δ_{b} can also be written as $\delta_{\mathrm{s}} = T/T_{\mathrm{s}}$ and $\delta_{\mathrm{b}} = T/T_{\mathrm{b}}$. Here T is the tidal period and T_{s} and T_{b} are time scales related to the suspended load and bedload mechanism, respectively. Both δ_{s} and δ_{b} should be small in order for the tidal averaging procedure to be applicable.

The corresponding boundary conditions become

$$\zeta = \cos t + \frac{\beta}{2}\cos(2t+\phi) \qquad \text{at } x = 0 \tag{13}$$

$$(1 - h + \epsilon\zeta)u = 0 \qquad \text{at } x = 1 \tag{14}$$

$$\lim_{\mu\to 0} C(x,t,\mu) = C(x,t,\mu = 0) \qquad \text{at } x = 0 \tag{15}$$

$$\epsilon u C - \mu C_x = 0 \qquad \text{at } x = 0 \tag{16}$$

$$h_t = 0 \qquad \text{at } x = 0 \tag{17}$$

$$F = 0 \qquad \text{at } x = 1 \tag{18}$$

Thus the tidal forcing at the entrance of the embayment consists of a basic tide and a first overtide. The relative strength of the overtide compared to the leading order tide is $\beta/2$ and ϕ is the phase difference between the two tidal components.

2.3 Solving the Model

According to (8) the elevation of the sea surface is independent of x in first order. This means that the surface excursions are determined by the excursion at the open end. With the boundary condition (13) for the free surface elevation, (7) can be solved explicitly which yields the velocity field

$$u(x,t) = \frac{(x-1)}{1 + \epsilon\left[\cos t + \beta/2\cos(2t+\phi)\right] - h}\;(\sin t + \beta\sin(2t+\phi)) \tag{19}$$

As can be seen for finite values of ϵ mass conservation results in the internal generation of overtides, which will also occur in case that the parameter $\beta = 0$. Using (19) in (9) the concentration can be computed. Finally the substitution of the solutions for u and C in (11) yields a net sediment flux which can be expressed as $F = F(h, h_x; a, \epsilon, \mu, \beta, \phi, \delta_{\mathrm{s}}, \delta_{\mathrm{b}})$. Thus (10) becomes a single partial differential equation for h which is of the advection diffusion type. In general, this procedure is difficult to carry out. Therefore we first estimate characteristic values of our model parameters for relatively short and deep embayments, for which (8) holds. As an example, consider the main channel of the Frision inlet system (Wang *et al.*, 1992). It has an approximate length of 20 km and a depth of 10 m. The forcing is due to the M_2 tide and the M_4 overtide contribution is rather strong. The sediment in the channel is fine sand with a grain size of $2\cdot 10^{-4}$ m. A typical value for the horizontal diffusion coefficient is $\mu_\star \sim 100\,\mathrm{m}^2\mathrm{s}^{-1}$, as discussed in *e.g.* (Ridderinkhof & Zimmerman, 1992). Using the information presented in (Dyer, 1986; Rijn, 1993) other quantities can be computed, such as the settling velocity, erosion coefficient α, etc.. They are listed in the first part of table 1.

Using (12), characteristic values for the parameters fo the nondimensional model are found, which are also shown in table 1. First of all it appears that both the

Quantities in the dimensional model		
$H \sim 10$ m	$L \sim 2 \cdot 10^4$ m	$\sigma \sim 1.4 \cdot 10^{-4}\ \mathrm{s}^{-1}$
$\hat{\zeta} = \frac{HU}{\sigma L} \sim 1.5$ m	$\kappa_{\mathrm{v}} \sim 0.1\ \mathrm{m}^2\,\mathrm{s}^{-1}$	$\mu_\star \sim 10^2\ \mathrm{m}^2\,\mathrm{s}^{-1}$
$d_{\mathrm{s}} \sim 2 \cdot 10^{-4}$ m	$w_{\mathrm{s}} \sim 2 \cdot 10^{-2}\ \mathrm{m\,s}^{-1}$	$\gamma \sim 4 \cdot 10^{-3}\ \mathrm{s}^{-1}$
$u_{\mathrm{c}} \sim 0.3\ \mathrm{m\,s}^{-1}$	$\rho_{\mathrm{s}} \sim 2650\ \mathrm{kg\,m}^{-3}$	$p \sim 0.4$
$\kappa_* \sim 2$	$\alpha \sim 10^{-2}\ \mathrm{kg\,s\,m}^{-4}$	$\hat{s} \sim 3 \cdot 10^{-6}\ \mathrm{m}^2\,\mathrm{s}^{-1}$
Parameters in the nondimensional model		
$\epsilon \sim 0.15$	$a \sim 0.04$	$\mu \sim 1.8 \cdot 10^{-3}$
$\kappa \sim 1 \cdot 10^{-3}$	$b \sim 3$	
$\delta_{\mathrm{s}} \sim 8 \cdot 10^{-4}$	$\delta_{\mathrm{b}} \sim 5.4 \cdot 10^{-7}$	
$\beta \sim 0.5$	$\phi \sim 7°$	

Table 1: Quantities and parameter values for the Frisian inlet system.

parameters δ_{s} and δ_{b} are very small, which justifies the application of a tidally averaged model. In this case the suspended load transport dominates over the bedload transport, but for other embayments with coarses sand the opposite will occur. It will be assumed that either bedload or suspended load is the main transport mechanism. Furthermore, it can be seen that the parameter ϵ, which measures the effects of nonlinear terms, is small. Hence we may expand the velocity u and concentration C in this small parameter, resulting in approximate solutions for the bed profile h. We will also use the observation that the parameters a and μ are often small in order to estimate the various contributions to the sediment flux F.

The following physically interesting cases will be studied:

- No overtide present: The parameter $\beta = 0$
  - advectively dominated suspended load transport: $a\epsilon^2 \gg \mu$ and $\delta_{\mathrm{b}} \ll \delta_{\mathrm{s}}$. The sediment flux is given by
  $$F = \delta_{\mathrm{s}} \epsilon^2 a^2 F_{\mathrm{sa}} + \text{h.o.t.}$$
  - diffusively dominated suspended load transport: $a\epsilon^2 \ll \mu$ and $\delta_{\mathrm{b}} \ll \delta_{\mathrm{s}}$. The sediment flux is given by
  $$F = \delta_{\mathrm{s}} a \mu F_{\mathrm{sd}} + \text{h.o.t.}$$
  - combined suspended load transport: $a\epsilon^2 \sim \mu$ and $\delta_{\mathrm{b}} \ll \delta_{\mathrm{s}}$. The sediment flux is given by
  $$F = \delta_{\mathrm{s}} \left[a\mu F_{\mathrm{sd}} + \epsilon^2 a^2 F_{\mathrm{sa}} \right] + \text{h.o.t.}$$
  - bedload transport: $\delta_{\mathrm{b}} \gg \delta_{\mathrm{s}}$ with sediment flux
  $$F = \delta_{\mathrm{b}} F_{\mathrm{db}} + \text{h.o.t.}$$

- Overtide present and relevant for the dynamics: The parameter $\beta \neq 0$
  - advectively dominated suspended load transport: $a\epsilon^2 \gg \mu$, $2\beta|\sin(\phi)| \gg 3a\epsilon$ and $\delta_{\rm b} \ll \delta_{\rm s}$. The second condition is necessary to study the effect of the overtide. The sediment flux is given by

$$F = \delta_{\rm s}\left[a\beta\epsilon F_{\rm sao} + \epsilon^2 a^2 F_{\rm sa}\right] + \text{h.o.t.}$$

  - diffusively dominated suspended load transport: $a\epsilon^2 \ll \mu$, $\beta\epsilon \ll \mu$ and $\delta_{\rm b} \ll \delta_{\rm s}$. The second condition states that even if an overtide is present, the diffusive effects are more important than the advective effects due to an overtide. The sediment flux is given by

$$F = \delta_{\rm s} a\mu F_{\rm sd} + \text{h.o.t.}$$

    Furthermore, it is assumed that $\mu\beta \gg \epsilon|\sin(\phi)|$ (this is highly unrealistic). With this choice, the leading order correction is given by the $a\mu\beta^2$ contribution:

$$F = \delta_{\rm s} a\mu\left(F_{\rm sd} + \beta^2 F_{\rm sdo}\right) + \text{h.o.t.}$$

  - combined suspended load transport: $a\beta\epsilon \sim \mu$, $\delta_{\rm b} \ll \delta_{\rm s}$. We assume that $\beta \gg a\epsilon$. The sediment flux is given by

$$F = \delta_{\rm s}\left[a\beta\epsilon F_{\rm sao} + a\mu F_{\rm sd}\right] + \text{h.o.t.}$$

    The system of table 1 satisfies the conditions of this case.
  - bedload transport: $\delta_{\rm b} \gg \delta_{\rm s}$ with sediment flux

$$F = \delta_{\rm b}\left[F_{\rm bd} + \beta F_{\rm abo}\right] + \text{h.o.t.}$$

The subscript a of the flux components denotes that the flux is related to advective processes. The subscripts d, s, b and o denote fluxes due to diffusive processes, suspended load processes, bedload processes, and the introduction of an overtide respectively.

Explicit expressions for the different flux contributions and the corresponding bedform behaviour will be given in the appropriate sections.

3 Simple Harmonic Tidal Forcing

In this section, the case that the parameter $\beta = 0$. Thus the forcing is represented by only one component of the tidal potential which excludes the possibility of modulations like spring–neap cycles. Furthermore higher harmonics which may be indirectly excitated by tide–topography effects and nonlinear terms in the equations of motion outside the domain of consideration are not taken into account. However, overtides are generated internally due to mass conservation, as can be seen from the solution for the velocity field:

$$u(x,t) = \frac{(x-1)\sin(t)}{1+\epsilon\cos(t)-h} \tag{20}$$

We will see that by taking only one tidal component into account significant differences between the behaviour of the bottom in the suspended load and bedload model are found.

3.1 Suspended Load Model

In this section, it is assumed that $\delta_{\mathrm{b}} \ll \delta_{\mathrm{s}}$ and hence that the dominant transport mechanism is described by the suspended load model only, neglecting the bedload transport mechanism.

3.1.1 Advectively Dominated Transport

We first consider the transport due to advective processes. Hence we neglect diffusion completely by putting the diffusion coefficient μ equal to zero in the concentration equation. This case is also important to generate the boundary condition for the concentration at $x = 0$ for arbitrary μ, as can be seen from (15). In this case the concentration C can be easily obtained, since the concentration equation is of the hyperbolic type. Using the method of characteristics it appears that the solution is determined by specifying initial conditions, since $t = 0$ is a curve that intersects all characteristics. This implies that the non–transient part of the solution can be constructed by straightforward means.

Since the expansion in the small parameter ϵ of the velocity can be made explicitly, (9) can be used to find the expansions for the concentration C. From the results of appendix B it follows that

$$C(x=0) = \frac{1}{2} - \frac{a}{1+4a^2}\left[\frac{1}{2a}\cos(2t)+\sin(2t)\right] + \mathcal{O}(\epsilon) \tag{21}$$

This yields the boundary condition on C at $x = 0$.

The sediment flux for $a \ll 1$ (which seems realistic according to table 1) becomes

$$F = -\frac{9}{8}\delta_{\mathrm{s}} a^2 \epsilon^2 \left(\frac{x-1}{1-h}\right)^3 \left(\frac{x-1}{1-h}\right)_x \tag{22}$$

From (10) and (18) it follows that an equilibrium bottom profile ($h_t = 0$) should obey $F = 0$ in the entire embayment. From the result shown above, it follows that $h_{\mathrm{eq}} = x$ is a stationary solution. However, the relevance of this result is limited since it cannot be reached from arbitrary initial conditions. This is because at the solid boundary $x = 1$ the velocity is zero and hence no net sedimentation occurs at this position. Therefore it is important to include diffusive transports as well.

3.1.2 Diffusively Dominated Transport

In this subsection we consider the limit that advective transport can be neglected compared to diffusive transport. In that case the net sediment flux in (9) and (11) can be approximated as

$$F = -\delta_s a\mu < C_0 >_x \tag{23}$$

where C_0 is the solution for the concentration equation (9) for $\epsilon = 0$. In appendix C the residual part $< C_0 >$ is expressed as a power series in the parameter $a\mu$, which appears to be a small parameter for the embayments we study (see table 1). Substitution of (58) of appendix C in (23) yields the bottom evolution equation

$$h_t = \delta_s \frac{a\mu}{2} \left(\frac{x-1}{1-h}\right)^2_{xx} \tag{24}$$

where terms of order $a^2\mu^2$ and higher are neglected. This yields the equilibrium bottom profile

$$h_{\rm eq} = x \tag{25}$$

It should be remarked that near $x = 1$ the condition $|1-h| \gg |\epsilon\zeta|$ is no longer satisfied. Strictly spoken, the model is not valid anymore in this region but nonetheless solutions for the transport and concentration are regular everywhere. Note that this equilibrium can always be reached since as $x = 1$ the sedimentation function is not necessarily zero.

To investigate the linear stability, we introduce a long time scale $\tau = \mu a \delta_{\rm s} t$ and perturb the equilibrium profile (25) with an arbitrary function $\tilde{h}(x,\tau)$ that satisfies the boundary condition $\tilde{h}(x = 0, \tau) = 0$ and the condition that the perturbed flux $\tilde{F}(x,\tau)$ is zero at $x = 1$. Thus substitute $h = h_{\rm eq} + \tilde{h}$ in (24) and linearize the equation. The equation allows solutions of the type

$$\tilde{h} = g(x)\exp(\omega\tau) + \text{c.c} \tag{26}$$

where $g(x)$ and ω are solutions of the eigenvalue problem

$$g_{xx} + 2\frac{g_x}{1-x} + \left[\frac{2}{(1-x)^2} - \frac{\omega(1-x)}{2}\right] g = 0 \tag{27}$$

In appendix A it is demonstrated that the only frequencies which give a non–trivial perturbation satisfying (27) and the imposed conditions on $\tilde{h}$ satisfy

$$J_{-\frac{1}{3}}(\frac{2}{3}\sqrt{-\omega}) = 0 \tag{28}$$

where $J_{-\frac{1}{3}}$ is the first order Bessel function of index $-\frac{1}{3}$. Hence the eigenfrequencies ω correspond to the zeroes of the Bessel function. Since the index of the Bessel function is real and larger than -1, all eigenfrequencies ω are real and negative (Abramowitz & Stegun, 1965) and hence equilibrium profile (25) is asymptotically linear stable. The corresponding eigenfunctions are given by

$$\tilde{h}(x) = A(1-x)^{\frac{3}{2}} J_{-\frac{1}{3}}\left(\frac{2}{3}\sqrt{-\omega}(1-x)^{\frac{3}{2}}\right)\exp(\omega\tau) \tag{29}$$

where A is an arbitrary amplitude. In figure 2 the evolution of an initially flat bottom towards the equilibrium profile as given by (25) is shown.

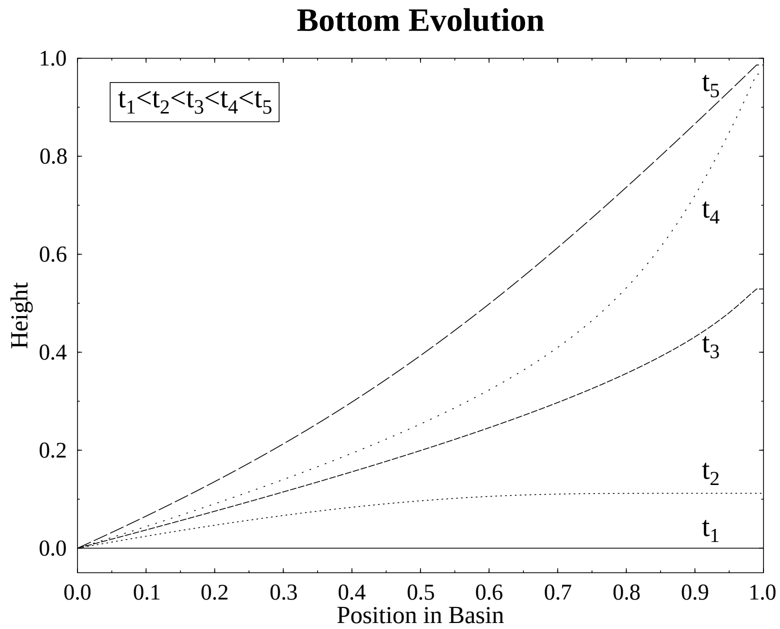

Figure 2: Evolution of an initially flat bottom towards equilibrium in the diffusively dominated case. The timesteps taken are on the morphological time scale $\tau = \mu a \delta_s$ with $t_1 = 0$, $t_2 = 1\tau$, $t_3 = 3\tau$, $t_4 = 5\tau$ and $t_5 = 8\tau$.

3.1.3 Combined Diffusive and Advective Transport

As shown in appendix B the leading order advective sediment transport is of order $\delta_s a^2 \epsilon^2$, whereas the leading order diffusive transport is of order $\delta_s a\mu$. Considering realistic values of the parameters $a\epsilon$ and μ it is obvious that for the tidal embayments we consider both transports will be of the same order. Thus it is interesting to combine both mechanisms in an overall model. Retaining only the leading order diffusive and advective transport, the bottom evolution term is given by

$$h_t = \delta_s \left\{ \frac{9}{8} a^2 \epsilon^2 \left[\left(\frac{x-1}{1-h}\right)^3 \left(\frac{x-1}{1-h}\right)_x \right]_x + \frac{a\mu}{2}\left(\frac{x-1}{1-h}\right)^2_{xx} \right\} \tag{30}$$

This equation is based on (24) and (22). The equilibrium profile is $h_{\mathrm{eq}} = x$. If we introduce the slow time $\tau = a^2\epsilon^2\delta_{\mathrm{s}}t$ and investigate the stability properties of this equilibrium, we again find that the perturbations are of the type (26), where g is the solution of the eigenvalue problem

$$g_{xx} + 2\frac{g_x}{1-x} + \left[\frac{2}{(1-x)^2} - \frac{\omega}{\frac{9}{8}+\hat{\mu}}(1-x)\right] g = 0$$

with boundary conditions and $\hat{\mu} = \mu/(a\epsilon^2)$. Using the results from appendix A and the discussion following (27), it is found that the equilibrium profile is stable.

In figure 3 the bottom evolution in the case that the diffusive and advective transport contributions are of comparable order is shown. The behaviour now contains elements of both the advectively and diffusively controlled case (Compare with figure 2 where only diffusive transport is taken into account). The advective character is seen by noting the front formation as the sediment moves into the basin.

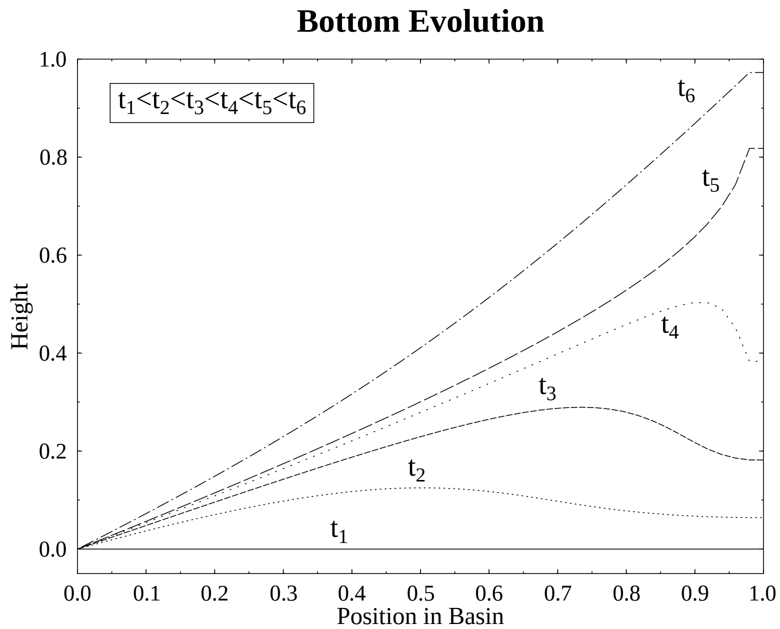

Figure 3: Evolution of an initially flat bottom towards equilibrium in the case that advective and diffusive transport contributions are of the same order of magnitude. The timesteps taken are on the morphological time scale $\tau = a^2\epsilon^2\delta_{\mathrm{s}}$ with $t_1 = 0$, $t_2 = 2\tau$, $t_3 = 5\tau$, $t_4 = 8\tau$, $t_5 = 10\tau$ and $t_6 = 17\tau$.

3.2 Bedload Model

In this section, it is assumed that the main transport mechanism is bedload transport and that suspended load transport can be neglected. Hence $\delta_{\mathrm{s}} \ll \delta_{\mathrm{b}}$ in (11). Note that when suspended load transport is neglected, the concentration C and sedimentation function S need not be calculated.

The bottom evolution equation is given by

$$h_t = -\delta_{\rm b} \left\langle \frac{\partial}{\partial x} \left[|u|^b \left(\frac{u}{|u|} - \kappa h_x \right) \right] \right\rangle \tag{31}$$

Define the long time scale $\tau = \delta_{\rm b} t$. The volumetric sediment transport consists of an advective part and a diffusive part. The velocity field u is given by (20). Since in this case u is anti–symmetric in t, it is clear that the advective part of the volumetric sediment transport is zero on average in all orders of the parameter ϵ. Hence the averaged bottom evolution equation to leading order in ϵ is given by

$$h_\tau = \kappa B(b) \frac{\partial}{\partial x} \left[\left| \frac{x-1}{1-h} \right|^b h_x \right] + \tag{32}$$

with

$$B(b) = \frac{1}{2\pi} \int_0^{2\pi} |\sin t|^b \; dt$$

with $B(b) \geq 0$ for all b.

Again we have as boundary conditions that the sediment flux $F(x = 1, \tau) = 0$ and $h(x = 0, \tau) = 0$ in equilibrium. The only equilibrium profile that satisfies these conditions is the flat bottom

$$h(x) = 0 \tag{33}$$

(note that the boundary condition (18) is not satisfied if we would allow $h_{\rm eq}(x) = x$). This is not surprising since (32) is a diffusive equation as only sediment transport due to gravitational bed slope effects is described. For the stability analysis we refer to section 4.2 where a more complicated case is discussed. Thus an equilibrium completely different from that in the case of suspended load transport is found.

Note that the present bedload model suffers from the problem that there is no net sedimentation at the solid boundary $x = 1$ because the velocity vanishes at this position. In order to obtain bed evolutions at $x = 1$ it is possible to extend the flux in (11) with a contribution $-\lambda h_x$, which models the rolling of particles on a sloping bed. The parameter λ is assumed to be small with respect to $\delta_{\rm b}$ such that this mechanism is only effective near $x = 1$ where bed slopes can become extremely large. The additional term is used in our numerical simulations with the bedload model, as discussed in section 4.2.

4 Introducing An Overtide

Instead of only considering the leading order tide, higher harmonics can be introduced. These higher harmonics are called the overtides. As discussed in section 2.1 they may be generated by interaction of the basic tide with the spatial geomorphology of the coastal sea to which the tidal tidal embayment is connected. Furthermore, overtides are excitated by self–interaction of the basic tide (Nihoul & Ronday, 1975). We only take the first overtide into account which results in free surface elevations at the entrance of the tidal embayment described by (13). The corresponding velocity field is given by (19). We will now analyze the behaviour of the model in case the prescribed overtides in the forcing of the entrance of the embayment significantly affect the dynamics.

4.1 Suspended Load Model

4.1.1 Advectively Dominated Transport

In this section, the diffusion coefficient μ equals zero. This limit is needed to obtain the boundary conditions for C at the entrance of the tidal embayment.

The solution method is equivalent to that used in section 3.1.1 for simple harmonic forcing. Thus the velocity (19) and concentration C are expanded in power series of the small parameter ϵ. Explicit expressions for the boundary condition on C at the entrance can be derived from the results of appendix B. Note that in this case the advective flux F at the entrance of the embayment is given by $< u_0 C_0 >$, see appendix B. This yields $F \simeq \frac{3}{4}\beta \sin\phi$, thus for $0° < \phi < 180°$ there is net import of sediment whereas for $-180° < \phi < 0°$ there will be net export of sediment. In these cases no equilibrium will exist.

4.1.2 Diffusively Dominated Transport

The derivation of the bottom evolution equation is similar as was done in section 3.1.2. We neglect the contribution resulting from advective transport compared to diffusive transport. Next we solve the concentration equation (9) to zeroth order in ϵ, using the velocity profile as given by (19). This leads again to an integral expression for the bottom evolution equation which, with the realistic assumption that $a\mu \ll 1$, reduces in the leading order to

$$h_t = \delta_s \frac{a\mu}{2}\left(1+\beta^2\right)\left(\frac{x-1}{1-h}\right)^2_{xx} \tag{34}$$

In deriving this equation, results from appendix C have been used. Note that in order to let the diffusive flux of $\mathcal{O}(\delta_{\mathrm{s}}\dashv\mu\beta^{\in})$ dominate over the advective flux, which is $\mathcal{O}(\delta_{\mathrm{s}} a\epsilon\beta\sin\phi)$ (see appendix B), we have to assume that $\mu\beta \gg |\epsilon\sin\phi|$ which is not realistic for the embayment of table 1.

If we introduce as the long time scale $\tau = \mu a \delta_s t$, the flux is given by

$$\begin{aligned} F(x,\tau) &= F_{\mathrm{sd}} + \beta^2 F_{\mathrm{sdo}} \\ &= -\frac{1}{2}(1+\beta^2)\left(\frac{x-1}{1-h}\right)^2_x \end{aligned}$$

and our equilibrium is given by

$$h_{\mathrm{eq}} = x$$

The flux and equilibrium profile are exactly the same as studied in section 3.1.2. Therefore, the equilibrium profile is stable. Due to increased diffusion, the equilibrium is reached faster. This was to be expected because the only effect of the overtide is to the increase the diffusion coefficient, resulting in faster diffusive transport.

4.1.3 Combined Diffusive and Advective Transport

In this section, the situation that the $a^2\beta\epsilon$–term in the advective transport and the $a\mu$ diffusive contribution are of the same order is studied. All other contributions are assumed to be negligible. The bottom evolution equation reads

$$h_\tau = \left[\frac{1}{2}\left(\frac{x-1}{1-h}\right)^2_{xx} + D\left(\frac{x-1}{1-h}\right)^3_x\right] \tag{35}$$

with

$$\tau = \delta_{\mathrm{s}} a\mu$$

and

$$D = \frac{3}{4}\frac{\epsilon\beta\sin(\phi)}{\mu} \tag{36}$$

which compares the relative strength of advective and diffusive transport. These results follow from (35) and (56) in appendix B. Since it was assumed that these effects were almost of equal strength, $|D| \simeq 1$. If $|D| \not\simeq 1$, one should refer to either the advectively or the diffusively dominated case instead of to this mixed case.

The equilibrium profile that gives a zero sediment flux at $x = 1$ is given by

$$h_{\mathrm{eq}} = 1 - (1-x)(1-Dx) \tag{37}$$

Note that the only physically relevant equilibrium profiles are given by $D \leq 1$. If $D > 1$, the equilibrium profile would exceed the water level. This is not allowed by our model. Obviously in this case the net import of sediment due to advective processes (because $\sin\phi > 0$) can no longer be compensated by net export caused by diffusive transport. As a consequence the embayment partly fills up, such that it length becomes smaller, velocities reduce, the scaled diffusion coefficient μ becomes larger and a new equilibrium can be found. In figure 4 some equilibrium profiles for different values of D are plotted.

To study the stability of the physically allowed equilibrium profiles, write the perturbed bottom profile as

$$h(x,\tau) = h_{\mathrm{eq}} + \tilde{h}$$

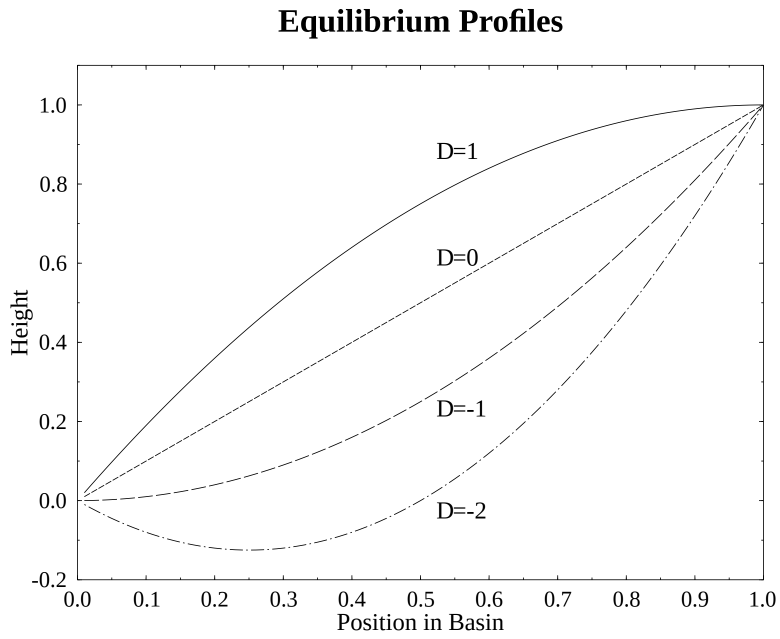

Figure 4: Equilibrium profiles in the advection–diffusion case with an overtide present. The parameter D refers to the ratio of advective and diffusive sediment transport.

This profile is put in the bottom evolution equation and linearized with respect to $\tilde{h}$. This results in the perturbed evolution equation

$$(1-x)\frac{\partial}{\partial t}f = \frac{\partial}{\partial x}\left[\frac{f_x}{(1-Dx)^3}\right] \tag{38}$$

with

$$f(x,\tau) = \frac{\tilde{h}}{1-x}$$

Write $f_t = \omega f$ where ω is the (complex) growth rate of the perturbation. Define the inner product

$$< g, h >_D = \int_0^1 (1-x) g\bar{h} dx$$

and the operator

$$\mathcal{L}_D = \frac{1}{1-x}\frac{\partial}{\partial x}\frac{1}{(1-Dx)^3}\frac{\partial}{\partial x}$$

With this inner product, it can be shown that

$$< \mathcal{L}_D g, h > = < g, \mathcal{L}_D h >$$

and therefore that all eigenvalues ω of (38) are real. Multiply (38) with f and integrate from $x=0$ to $x=1$. After integration by parts one finds that

$$\frac{1}{2}\int_0^1 (1-x) f^2 \, dx = -\int_0^1 \frac{f_x^2}{(1-Dx)^3}\, dx \tag{39}$$

Here it has been used that $\tilde{h} \sim (1-x)^2$ near $x = 1$ (as follows from analysing the equation near $x = 1$) and $\tilde{h}(x = 0) = 0$. It is seen that the right–hand side of (39) is non–positive whenever $D \leq 1$. This is exactly the physically relevant parameter region. Because it is known that the eigenvalues of the problem are real, the physically relevant equilibrium profiles as defined in (37) are stable. In figure 5 the evolution of the bottom profile is shown in the case that $D = -2$.

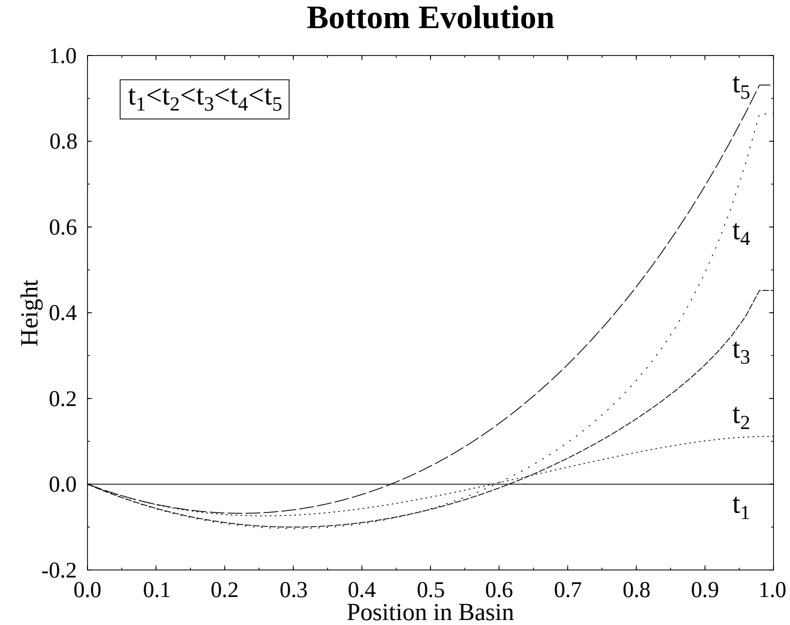

Figure 5: Bottom profile at different times during the bottom evolution of the advection–diffusion case with overtide with $D = -2$. The timesteps taken are on the morphological time scale $\tau = \mu a \delta_s$ with $t_1 = 0$, $t_2 = 1\tau$, $t_3 = 3\tau$, $t_4 = 5\tau$ and $t_5 = 8\tau$.

If $D = 1$, the equation can be solved analytically. Write the perturbed equilibrium as

$$h(x, \tau) = h_{\text{eq}} + g(x) \exp(\omega\tau)$$

resulting in the perturbed bottom evolution equation, which is given by

$$g_{zz} - 5\frac{g_z}{z} + \left(\frac{5}{z^2} - \omega z^4\right) g = 0$$

Using the method as described in appendix A, it is found that the growth rate ω of the perturbations is found by solving

$$J_{\frac{2}{3}}\left(\frac{1}{3}\sqrt{-\omega}\right) = 0$$

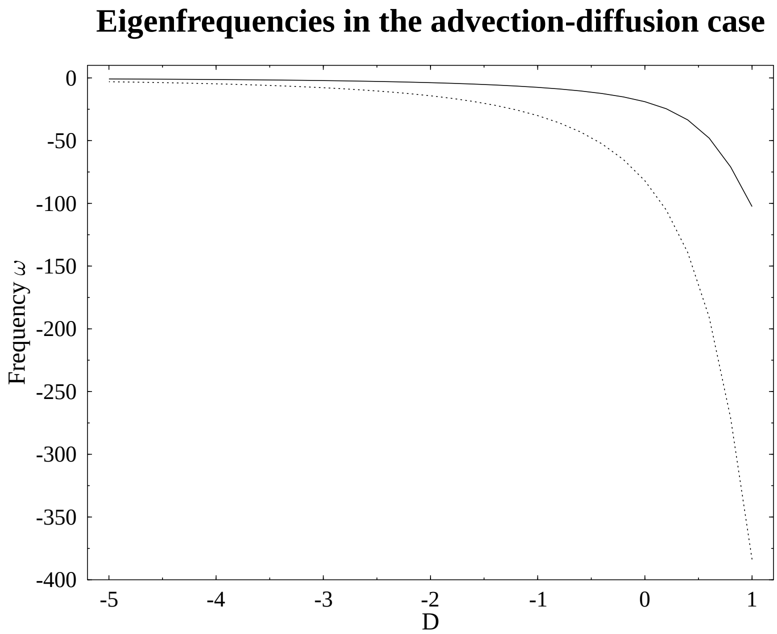

Figure 6: Growth rates as function of the parameter D.

These eigenfrequencies ω are used as starting values to find numerically the eigenfrequencies of (38) for other values of the parameter D. The results are presented in figure 6 where the eigenfrequencies are plotted as function of D.

As was predicted by the variational method, the equilibrium profile (38) is linearly asymptotic stable.

Note that if $D = 0$, the evolution equation reduces to the purely diffusive case. With this in mind, it is seen that if the tidal embayment is flood dominated ($0° \leq \phi \leq 180°$), the advective contribution to the transport is stabilizing (the combined advection–diffusion transport model has a smaller growth rate than the purely diffusive model). If the tidal embayment is ebb dominated ($-180° \leq \phi \leq 0°$), the advective term is destabilizing.

4.2 Bedload Model

If we introduce an overtide in the bedload model, the average of the advective part of the volumetric sediment flux in (32) is not zero, unless the phase difference ϕ between the two tides is zero or 180 degrees. A special case of a slightly different model is studied in (Dongeren & de Vriend, 1994). The leading order diffusive contribution (*i.e.* the contribution coming from the κh_x term) is of $\mathcal{O}(\epsilon^0)$, the leading order advective contribution (*i.e.* the contribution coming from the $u/|u|$ term) is of $\mathcal{O}(\epsilon^0\beta)$. These contributions can be calculated using the velocity profile as given by (19) and the bottom evolution equation (31), yielding in leading order

$$h_\tau = -\frac{\partial}{\partial x}\left\{\left[k(b,\beta,\phi) - \kappa B(b,\beta,\phi)\frac{\partial h}{\partial x}\right]\left|\frac{x-1}{1-h}\right|^b\right\} \tag{40}$$

with $\tau = \delta_{\mathrm{b}} t$,

$$k(b,\beta,\phi) = -\left\langle |\sin(t) + \beta\sin(2t+\phi)|^{b-1}\left[\sin(t) + \beta\sin(2t+\phi)\right]\right\rangle$$

and

$$B(b,\beta,\phi) = \left\langle |\sin(t) + \beta\sin(2t+\phi)|^{b}\right\rangle$$

In equilibrium, the sediment flux has to be zero on average. Therefore, the only equilibrium profile is given by

$$h_{\mathrm{st1}} = \frac{k(b,\beta,\phi)}{B(b,\beta,\phi)\kappa}x \tag{41}$$

Note that if

$$\frac{k(b,\beta,\phi)}{\kappa B(b,\beta,\phi)} \geq 1 \tag{42}$$

the equilibrium profile cannot be reached because the bottom profile would exceed the water level. Physically this case is similar to that discussed in section 4.1.3 for $D > 0$, *i.e.*, the diffusive transport cannot compensate for the advective transport.

The stability of the equilibrium solution (41) can be studied using the variational method. To this end, write

$$h(x,\tau) = h_{\mathrm{st1}}(x) + \tilde{h}(x,\tau)$$

with $\tilde{h}$ the perturbation on the equilibrium profile. Inserting this in (40) and linearizing with respect to $\tilde{h}$ yields the perturbed bottom evolution equation. It can be shown that the resulting operator is self adjoint and hence that all eigenvalues of h are real. Multiply the eigenvalue equation with $\tilde{h}$ and integrate over the tidal embayment length. This yields, after integration by parts (using that at the end of the tidal embayment $h(x=1)=1$)

$$\frac{1}{2}\frac{\partial}{\partial\tau}\int_0^1 \tilde{h}^2\,dx = -\kappa B(b,\beta,\phi)\int_0^1\left|\frac{x-1}{1-\frac{k(b,\beta,\phi)}{\kappa B(b,\beta,\phi)}x}\right|^b\left(\frac{\partial\tilde{h}}{\partial x}\right)^2 dx \tag{43}$$

Hence (41) is stable since $B(b,\beta,\phi) > 0$. In figure 7 the bottom profile is shown at subsequent times, starting from two different initial profiles. The parameter $k(b,\beta,\phi)/B(b,\beta,\phi)\kappa$ was set to a half.

It can be concluded that the parameter $k(b,\beta,\phi)/B(b,\beta,\phi)\kappa$ determines the behaviour of the tidal embayment. If this parameter is larger than one, meaning that

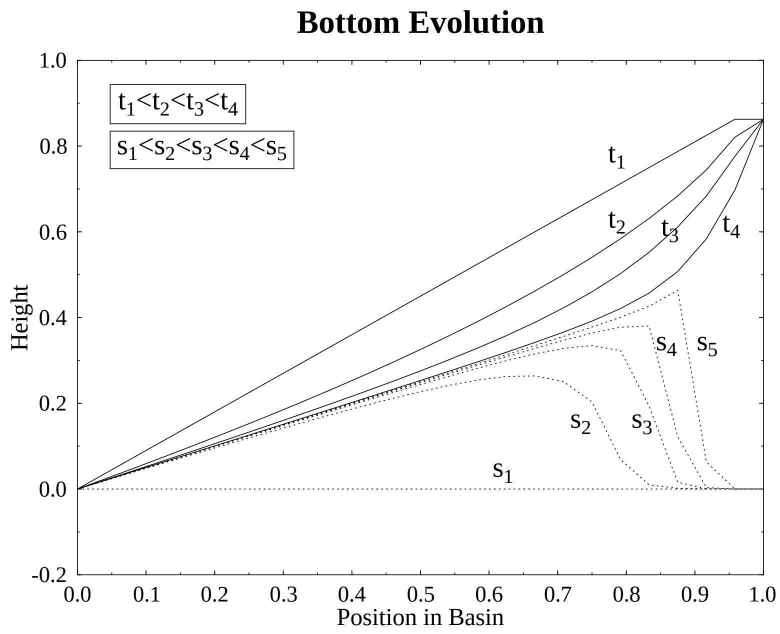

Figure 7: Time evolution of the bottom. The subsequent profiles are denoted by t_i for the initial profile $h(x,t=0)=0.9x$ and s_i for initial profile $h(x,t=0)=0$. The timesteps taken are on the morphological time scale $\tau=\delta_{\mathrm{b}}$ with $t_1=0$, $t_2=1\tau$, $t_3=3\tau$, $t_4=8\tau$, $s_1=0$, $s_2=1\tau$, $s_3=3\tau$, $s_4=5\tau$, $s_5=8\tau$.

diffusive effects cannot balance the advective fluxes, no equilibrium position is found and the embayment will fill up. This means that the length of the tidal embayment decreases until the situation that $k(b,\beta,\phi)/B(b,\beta,\phi)\kappa=1$ is reached. At that moment, the linear sloping bottom is stable. Thus a tidal flat area is formed until a situation is reached in which there is no net transport anymore. Hence the coupling between the tides determines the length of the tidal embayment. This phenomenon was found numerically in (Wang, 1992).

5 Conclusions

In this paper, we investigated the presence of equilibrium bottom profiles in tidal embayments which are short compared to the tidal wave length and which are driven by prescribed surface elevations at the seaward boundary. Relative deep embayments were considered for which the frictional time scale is at least of the order of the tidal period. This distinguishes our systems from the highly frictional embayments studied e.g. in (Friedrichs *et al.*, 1990; Friedrichs & Madson, 1992). It was assumed that the width of the tidal embayment was small compared to both its length and the Rossby deformation radius so that the model could be reduced to a one dimensional model. Since the tidal period is much shorter than the morphodynamical time scale, the method of averaging was used to separate the time scales. We investigated both leading order tidal forcing and forcing due to a leading order tide and its first overtide. It appears that overtides are also generated internally in the model due to mass conservation. The main conclusion is that stable equilibria can be found and that there are important differences between a morphodynamic model for a tidal embayment based on a suspended load transport mechanism and a bedload model.

If no overtide was considered, it was found that with sediment transport dominated by suspended load transport, the equilibrium profile that satisfied all boundary conditions represents a constantly sloping bottom. In the case of bedload transport, the bottom evolution equation reduced to a diffusion equation with the flat bottom as equilibrium profile. It turned out that all profiles were stable within the context of the one dimensional model.

In the case that an overtide was introduced in the forcing of the system, a wide variety of equilibrium profiles could be found, depending on the magnitude of the various parameters in the problem. It was demonstrated that not only the intensity of the overtide was important, but also its phase difference ϕ with the leading order tide. Although the changes of the equilibrium profiles in the suspended load case appeared to be profound, the change of equilibrium profile was most profound when bedload transport is considered. If an overtide was present, the bedload transport model resulted in a linear bottom profile whereas in the case with no overtide the flat bottom was the only equilibrium profile. Depending on the phase ϕ the tidal embayment could be exporting or importing sediment. The equilibrium profiles were all stable.

It appears that the equilibrium solutions of the one dimensional model are also solutions of the original two dimensional model except for the case that advective suspended load transport is considered in a system driven by overtides. However, their stability properties in the full model may be quite different compared with the one dimensional case because the perturbation have more degrees of freedom. Similar results in river–like problems (Schielen *et al.*, 1993) suggest the excitation of instabilities when a one dimensional model is extended to a two dimensional version. This will be investigated in a forthcoming paper. It is expected that the spatial structure of unstable perturbations will resemble in some sense observed channel–shoal systems in tidal embayments. Furthermore, it would be interesting to study effects of width variations in the channel geometry and include frictional terms in the momentum equations, as they are relevant in most realistic tidal embayments.

References

Abramowitz, M., & Stegun, I. A. 1965. *Handbook of mathematical functions.* New York: Dover Publications.

Aubrey, D. G., & Speer, P. E. 1985. A study of nonlinear tidal propagation in shallow inlet/estuarine systems. Part 1: Observations. *Est. Coastal Shelf Sci.*, **21**, 185–205.

Bruun, P., & Gerritsen, F. 1960. *Stability of coastal inlets.* Amsterdam: North Holland.

Csanady, G. T. 1982. *Circulation in the coastal ocean.* Dordrecht: Reidel.

Dongeren, A. R. van, & de Vriend, H. J. 1994. A model of morphological behaviour of tidal basins. *Coastal Eng.*, **22**, 287–310.

Dyer, K. R. 1986. *Coastal and estuarine sediment dynamics.* Chichester: John Wiley & Sons.

Dyer, K. R., & Soulsby, R. L. 1988. Sand transport on the continental shelf. *Ann. Rev. Fluid Mech.*, **20**, 295–324.

Fredsoe, J., & Deigaard, R. 1992. *Mechanics of coastal sediment transport.* Singapore: World Scientific.

Friedrichs, Carl T., & Aubrey, David G. 1994. Tidal propagation in strongly convergent channels. *J. Geophys. Res.*, **99**, 3321–3336.

Friedrichs, Carl T., Aubrey, David G., & Speer, Paul E. 1990. Impacts of relative sea–level rise on evolution of shallow estuaries. *Pages 105–123 of:* Cheng, R. T. (ed), *Residual currents of long–term transport.* New York: Springer–Verlag.

Friedrichs, C.T., & Madson, O.S. 1992. Nonlinear diffusion of the tidal signal in frictionally–dominated embayments. *J. Geophys. Res.*, **97**, 5637–5650.

Garret, C.J.R. 1975. Tides in gulfs. *Deep–Sea Res.*, **22**, 23–35.

Jonge, V. N. de. 1992. *Physical processes and dynamics of microphytobenthos in the Ems estuary (the Netherlands).* Ph.D. thesis, University of Groningen.

Krol, M. 1991. On a Galerkin–averaging method for weakly nonlinear wave equations. *Math. Appl. Sci.*, **11**, 649–664.

Nihoul, Jacques C., & Ronday, Francois C. 1975. The influence of the tidal stress on the residual circulation. *Tellus*, **27**, 484–489.

Parker, B. B. (ed). 1991. *Tidal Hydrodynamics.* New York: John Wiley & Sons.

Ridderinkhof, H., & Zimmerman, J. T. F. 1992. Chaotic stirring in a tidal system. *Science*, 1107–1111.

RIJN, L. C. VAN. 1993. *Principles of sediment transport in rivers, estuaries and coastal seas.* Amsterdam: Acqua Publ.

SANDERS, J. A., & VERHULST, F. 1985. *Averaging methods in nonlinear dynamical systems.* New York: Springer–Verlag.

SCHIELEN, R., DOELMAN, A., & DE SWART, H. E. 1993. On the nonlinear dynamics of free bars in straight channels. *J. Fluid Mech.*, **252**, 325–356.

SPEER, P. E., & AUBREY, D. G. 1985. A study of nonlinear tidal propagation in shallow inlet/estuarine systems. Part 2: Theory. *Est. Coastal Shelf Sci.*, **21**, 207–224.

WANG, Z. B. 1992. *Fundamental considerations on morphodynamic modelling in tidal regions. Part 1: Theoretical analysis and 1D computations.* Tech. rept. Waterloopkundig Laboratorium.

WANG, Z. B., LOUTERS, T., & DE VRIEND, H. J. 1992. A morphodynamic model for a tidal inlet. *Pages 235–245 of:* ARCILLA, A.S., & OTHERS (eds), *Computing Modelling in Ocean Engineering '91.* Rotterdam: Balkema.

ZIMMERMAN, J. T. F. 1981. Dynamics, diffusion and geomorphological significance of tidal residual eddies. *Nature*, 549–555.

A Stability Analysis Of Perturbed Profiles

In this appendix the stability of the equilibrium bottom profile $h_{\mathrm{eq}} = x$ will be studied. The bottom is perturbed with perturbations given by (26)

$$\tilde{h} = g(x)\exp(\omega\tau) + \mathrm{c.c} \tag{44}$$

resulting in a perturbed bottom evolution equation

$$g_{xx} + 2\frac{g_x}{1-x} + \left[\frac{2}{(1-x)^2} - f(\omega)(1-x)\right] g = 0 \tag{45}$$

where $f(\omega)$ is ω in the case of diffusively dominated transport and $\omega/(\frac{9}{8} + \hat{\mu})$ when advective and diffusive transport are combined. For clearity, take $f(\omega) = \omega$. The other case goes along the same line of thoughts.

First, define $z = 1 - x$ and $g(z) = z\psi(z)$ and rewrite the equation as

$$\psi_{zz} - \omega z \psi = 0 \tag{46}$$

which is the Airy equation. The solution of this equation can be given in terms of Bessel functions (Abramowitz & Stegun, 1965). The differential equation (46) is of the Sturm–Liouville type which has always real eigenvalues. Hence ω is real.

The final result for the bed topography becomes

$$\tilde{h} = z^{\frac{3}{2}}\left[AJ_{\frac{1}{3}}(\frac{2}{3}\sqrt{-\omega}z^{\frac{3}{2}}) + BJ_{-\frac{1}{3}}(\frac{2}{3}\sqrt{-\omega}z^{\frac{3}{2}})\right]e^{\omega\tau} + \mathrm{c.c.} \tag{47}$$

with A and B arbitrary complex constants.

To determine the constants, consider the special case that $B = 0$ and insert $\tilde{h}$ in the perturbed flux

$$\tilde{F} \sim -\left(\frac{\tilde{h}}{z^2} + \frac{\tilde{h}_z}{z}\right) = \left(\frac{\tilde{h}}{z}\right)_z$$

First, assume that $\omega > 0$. Using the behaviour of the Bessel functions near $z = 0$, one finds that

$$\tilde{F} \sim Ae^{-\frac{1}{3}i\pi} + \mathrm{c.c.}$$

Hence, the flux does not vanish at $z = 0$ unless $A\exp(-\frac{1}{3}i\pi) \in \mathbb{C}$. However, with this choice and the identities

$$\overline{J_\nu(z)} = J_\nu(\bar{z})$$

and

$$J_\nu(ze^{m\pi i}) = e^{m\nu\pi i}J_\nu(z)$$

with m an integer (see (Abramowitz & Stegun, 1965)), it can be shown that the perturbation is zero identically. The same can be done for $\omega < 0$. Therefore, we can put $A = 0$.

If $A = 0$, the flux vanishes at $z = 0$. This can be seen by noting that

$$z^{\frac{3}{2}} J_{\frac{1}{3}}(\frac{2}{3}\sqrt{-\omega} z^{\frac{3}{2}}) \sim z + \mathcal{O}(z^4)$$

This means that

$$\tilde{h} = B z^{\frac{3}{2}} J_{-\frac{1}{3}}(\frac{2}{3}\sqrt{-\omega} z^{\frac{3}{2}}) e^{\omega\tau} + \text{c.c.} \tag{48}$$

The boundary condition $h(x = 0) = 0$ will give us our set of eigenfrequencies. If $\omega > 0$ the condition that must be satisfied at $x = 0$ is

$$\left(B + \bar{B} e^{-\frac{1}{3} i\pi}\right) J_{-\frac{1}{3}}(\frac{2i}{3}\sqrt{\omega}) = 0 \tag{49}$$

again using the identities

$$\overline{J_\nu(z)} = J_\nu(\bar{z})$$

and

$$J_\nu(z e^{m\pi i}) = e^{m\nu\pi i} J_\nu(z)$$

Since $-1/3 > -1$ and real, all zeroes of the Bessel function are real, as was to be expected. In (49) the argument of the Bessel function is imaginary and hence the constant B must be chosen in such a way that the condition $\tilde{h}(x = 0) = 0$ is satisfied. However, with this choice of the constant B, it is seen, using (48), that $\tilde{h} = 0$ for all x. Therefore the only frequencies that give a non–trivial perturbation satisfying the boundary conditions satisfy

$$J_{-\frac{1}{3}}(\frac{2}{3}\sqrt{-\omega}) = 0 \tag{50}$$

Using again the argument that $\nu > -1$ and real, all zeros of the Bessel function are real. From this it follows that $\omega < 0$ and real and hence that the bottom profile is asymptotically linear stable.

If $f = \omega/(\frac{9}{8} + \hat{\mu})$, the case with combined advective and diffusive transport, the eigenfrequencies are found by solving

$$J_{-\frac{1}{3}}(\frac{2}{3}\sqrt{-\frac{\omega}{\frac{9}{8} + \hat{\mu}}}) = 0 \tag{51}$$

with the corresponding eigenfunctions

$$\tilde{h} = B z^{\frac{3}{2}} J_{-\frac{1}{3}}(s z^{\frac{3}{2}}) e^{\omega\tau} \tag{52}$$

with

$$s = \frac{2}{3}\sqrt{-\frac{\omega}{\frac{9}{8} + \hat{\mu}}}$$

B Advectively Dominated Transport

B.1 Simple Harmonic Tidal Forcing

In the case we have to solve (7)– (9) with $\mu = 0$, $\delta_{\mathrm{b}} = 0$ and the velocity field (20). Approximate solutions are constructed by expanding both the velocity and the concentration in the small parameter ϵ:

$$\begin{aligned} u &= u_0 + \epsilon u_1 + \ldots \\ C &= C_0 + \epsilon C_1 + \ldots \end{aligned}$$

The zeroth order concentration equation reads

$$aC_{0t} = u_0^2 - C_0 \tag{53}$$

with solution

$$C_0 = \left(\frac{x-1}{1-h}\right)^2 \left\{\frac{1}{2} - \frac{a}{1+4a^2}\left[\frac{1}{2a}\cos 2t + \sin 2t\right]\right\} \tag{54}$$

Since C_0 is T–periodic, it follows that

$$< u_0 C_0 >= 0$$

Hence the sediment flux becomes

$$F = \delta_{\mathrm{s}} a \epsilon^2 \langle u_0 C_1 + u_1 C_0 \rangle + \mathcal{O}(\epsilon^\ni)$$

By solving the first order equation for C_1, it finally follows that

$$\begin{aligned} F = \delta_{\mathrm{s}} \epsilon^2 \Bigg\{ & \frac{1}{4}\left(\frac{x-1}{1-h}\right)^3 \frac{1}{1-h}\left(\frac{a^2}{1+4a^2} - \frac{a^2}{1+a^2}\right) \\ & -\frac{3}{4}\left(\frac{x-1}{1-h}\right)^3 \frac{\partial}{\partial x}\left(\frac{x-1}{1-h}\right)\left[\frac{a^2}{1+a^2}\left(1+\frac{1}{2}\frac{1-2a^2}{1+4a^2}\right)\right]\Bigg\} \end{aligned} \tag{55}$$

B.2 Overtide

The difference with section B.1 is that the velocity field is given by (19). We use the same method as in section B.1 to solve the concentration equation. For small a we find for the $\mathcal{O}(\epsilon')$ concentration $C_0 \simeq u_0^2$ where $u_0 = u(\epsilon = 0)$. From this the boundary condition for C at $x = 0$ can be obtained. Thus $< u_0 C_0 > \simeq < u_0^3 >$ and this yields

$$< u_0 C_0 > \simeq -\frac{3}{4}\beta \sin(\phi)\left(\frac{x-1}{1-h}\right)^3$$

The corresponding sediment transport becomes

$$F = \delta_{\mathrm{s}} a\epsilon < u_0 C_0 > \simeq -\frac{3}{4}\delta_{\mathrm{s}} a\epsilon\beta \sin(\phi)\left(\frac{x-1}{1-h}\right)^3 \tag{56}$$

which is the result used in the text. Note that it only dominates the advective transport due to the basic tide, given in (22), in case $|\beta \sin\phi| \gg a\epsilon$. For the system of table 1, this condition is satisfied.

C Diffusively Dominated Transport

C.1 Simple Harmonic Tidal Forcing

The equations to be solved are (7)– (9) and (20) with $\epsilon = 0$, $\delta_{\rm b} = 0$. in this case the sediment flux reads $F = -\delta_s a\mu < C_0 >_x$, so only the stationary concentration profile has to be computed. It obeys

$$-a\mu \left\langle C_0 \right\rangle_{xx} + \left\langle C_0 \right\rangle = \frac{1}{2}\left(\frac{x-1}{1-h}\right)^2 \tag{57}$$

Since the parameter $a\mu \ll 1$ for most embayments (see e.g. table 1) a solution follows from the application of singular perturbation thechniques. Since the boundary condition (15) guarantees that there will be no diffusive boundary layer near $x = 0$ the solution of (57) is

$$< C_0 >= \frac{1}{2}\left(\frac{x-1}{1-h}\right)^2 + \mathcal{O}(a\mu) \tag{58}$$

which is the result used in the text. Note that it also obeys the boundary condition (16) at $x = 1$, hence it is a valid solution in the entire domain.

C.2 Overtide

The method of analysis is similar to that discussed in the previous section, except that the velocity field is given by (19). Solving the stationary concentration equation now yields

$$\left\langle C_0 \right\rangle = \frac{1}{2}\left(1+\beta^2\right)\left(\frac{x-1}{1-h}\right)^2$$

and the corresponding sediment flux is $F = -\delta_{\rm s} a\mu < C_0 >_x$.